Force Reflecting Bilateral Control of Master-Slave Systems in Teleoperation

A. ALFI[†], M. FARROKHI[†‡]

† Department of Electrical Engineering,
‡ Center of Excellence for Power System Automation and Operation
Iran University of Science and Technology, Tehran 16846-13114, IRAN

e-mails: a_alfi@iust.ac.ir, farrokhi@iust.ac.ir

Abstract. In this paper, a simple structure design with arbitrary motion/force scaling to control teleoperation systems, with model mismatches is presented. The goal of this paper is to achieve transparency in presence of uncertainties. The master-slave systems are approximated by linear dynamic models with perturbed parameters, which is called the model mismatch. Moreover, the time delay in communication channel with uncertainties is considered. The stability analysis will be considered for two cases: 1) stability under time delay uncertainties and 2) stability under model mismatches. For the first case, two local controllers are designed. The first controller is responsible for tracking the master commands, while the second controller is in charge of force tracking as well as guaranteeing stability of the overall closed-loop system. In the second case, an additional term will be added to the control law to provide robustness to the closed-loop system. Moreover, in this case, the local slave controller guarantees the position tracking and the local master controller guarantees stability of the inner closed-loop system. The advantages of the proposed method are two folds: 1) robust stability of the system against model mismatches is guaranteed and 2) structured system uncertainties are well compensated by applying independent controllers to the master and the slave sites. Simulation results show good performance of the proposed method in motion tracking as well force tracking in presence of model mismatches and time delay uncertainties.

Key words: Bilateral Teleoperation, Transparency, Force Reflection, Time Delay Systems.

1. Introduction

Master-slave teleoperation systems enable human interaction with environments that are remote, hazardous, or inaccessible to direct human contact, such as mining, sub sea exploration, and more recently in health care [1]. The main components of a teleoperation system are: 1) a set of two robotic manipulators, referred to as the "local master system" (or "master" for short) and the "remotely located slave system" (or "slave" for short), 2) the communication channel, 3) the human operator, and 4) the task environment.

In bilateral teleoperation, human operator applies force to the master in order to produce the desired output, which can be position or velocity. The output of master is transmitted to the slave through the communication channel to produce the desired force in the slave system that generates the position or velocity at the remote side, respectively. Due to the interactions between the slave system and its environment, a reaction force is generated, which is sent back as the reflecting force to the master to complete the closed-loop system. By feeding the reflecting force back to the master robot and then to the human operator, which is called force-reflecting control in teleoperation systems, the overall performance can be improved [2].

Based on the time-delay in communication channel and uncertainties in the task environment, there are two major issues in teleoperation systems: stability and performance. Transparency is the major criterion for performance of the teleoperation systems in presence of time delay in communication channel as well as stability of the closed-loop system. If the slave accurately reproduces the master's commands and the master correctly feels the slave forces, then the human operator experiences the same interaction as the slave would. This is called transparency in teleoperation systems [3].

The communication channel becomes an important issue when the distance between the master and the slave is too long. In this case, a time delay appears in information transmission that cannot be ignored. Due to this time delay, performance of the bilateral teleoperation systems can be degraded, which can even lead to instability of the remotely controlled manipulator. For the first time, Ferrel showed the instability of a teleoperation system with time delay [4]. In 1981, Vertut and Coiffet showed that stability of teleoperation systems with time delay could be achieved by decreasing bandwidth of the closed-loop system [5].

To overcome the time delay problem, various methods have been proposed in literatures. In 1989, Anderson and Spong stabilized the system against large, but constant time delay by using a passive model for transmission channel [6]. In 1991, Niemeyer and Slotine extended this result by introducing the concept of wave variable signals to stabilize the teleoperation system under unknown but constant time delay [7]. Further, in 1997, they used a filter in the wave variable signals that improved the error between the positions of master and slave by transmitting the integral of wave variable signals [8]. Kim et al. used force reflection and shared compliant control to improve the teleoperation tasks [9]. Buttolo et al. proposed model-based first-order sliding-mode controllers for both the local and the remote sites. Unfortunately, in addition to the high frequency signals problem, the teleoperation system becomes unstable with minor delays [10]. In 2005, Valdovinos et al. proposed higher-order sliding-mode impedance control to solve the chattering problem [11]. Leeraphan et al. proposed an adaptive gain to ensure a passive system for every time delay that adapts characteristic impedance. However, they did not investigate the transparency for their teleoperation system [12]. Zhu and Salcudean proposed an adaptive motion/force controller for unilateral or bilateral teleoperation systems

that can be applied to both position and rate control methods [13]. Munir and Book used the Kalman filter and a time-forward observer to predict the wave variables and to compensate for the time delays [14]. Hashtrudi-Zaad et al. analyzed transparency of the teleoperation system in presence of time delay using three-channel control method [15]; nevertheless, their method is difficult to realize. Yokokohji et al. proposed a control scheme that provides the ideal kinesthetic coupling such that it does not require any knowledge of the parameters of the human operator dynamics and the remote object [16]. Leung et al. modeled the time delay as a perturbation to the system, and designed the system to be robust against such perturbations using H_∞ optimal control as well as μ-synthesis [17]. Baier and Schmidt proposed a novel control strategy by using two-port lossless line theory for stabilization and transparency of bilateral teleoperation systems [18]. Ching and Book proposed bilateral teleoperation based on wave variable with adaptive predictor and direct drift control method [19].

Recently, Alfi and Farrokhi proposed a new structure for bilateral transparent teleoperation systems in presence of time delay [20-22]. To achieve complete transparency and stability in the proposed method, direct-force measurement-force reflecting control is employed at the local site. In the direct-force measurement-force reflecting control, the position/velocity signal is transmitted from the master to the slave. Then, using a force sensor, the reflected force from the environment is sent back in the opposite direction to produce feedback signals, which is applied to the master in order to give the operator a sense of what is happening in the remote site [1].

The goal of this paper is two folds: 1) developing a simple structure for scaled bilateral teleoperation systems with arbitrary motion/force scaling, and 2) developing conditions for robust stability of the proposed structure in presence of uncertainties in the dynamics of teleoperation systems.

The stability analysis of the proposed structure is considered for two cases: 1) stability against the time delay uncertainties and 2) stability against model mismatches. In the first case, two local controllers are designed. The first controller is responsible for tracking the master commands. The second controller is in charge of force tracking as well as guaranteeing the stability of the overall closed-loop system. In the second case, a robust control term will be added to the control law to provide stability robustness to the closed-loop system. Moreover, in this case, the local slave controller guarantees the position tracking and the local master controller guarantees stability of the inner closed-loop control system. In this way, the slave follows the master with good accuracies despite model mismatches. In addition, in the core of the proposed control structure, an identification algorithm is developed, which, in addition to predicting the time-delay parameter, makes the closed-loop system virtually independent of the time delay. Moreover, as a result, the forward and the backward time delays need not to be identical in the proposed structure. In the rest of this paper, whenever it is referred to “the time delay”, it means “the time delay in communication channel”.

This paper is organized as follows. In Section 2, the basic proposed control method is discussed. Section 3 describes design of the controllers. Analytical work about the stability of the proposed structure is given in Section 4. Section 5 shows the simulation results. Finally, conclusions will be drawn in Section 6.

2. The Basic Proposed Control Scheme

The basic proposed control structure is shown in Figure 1. In this Figure, G, C and y denote the transfer functions of the local systems, the local controllers, and the outputs, respectively. The subscripts *m* and *s* denote the master and the slave, respectively. Moreover, T_{ms} and T_{sm} indicate the forward (i.e. from the master to the slave) and the backward (i.e. from the slave to the master) time delays, respectively. F_e is the force exerted on the slave from its environment, Z_e is impedance of the environment, F_h is the force applied to the master by the human operator, K_p and K_f are the arbitrary motion and force scaling factors, respectively, F_s is the input force applied to the slave, and F_r is the reflected force.

The following assumptions have to be stated first:

ASSUMPTION 1. The slave system acts in a non-free task environment.

ASSUMPTION 2. The forward and the backward time delays are unknown and not identical.

ASSUMPTION 3. The contact force is measurable and available for the local controller. Moreover, direct-force measurement-force reflecting control is used at the local site.

ASSUMPTION 4. In order to give the operator the force sensation, the contact force is sent back, as the reflecting force, to the master robot.

The main goals of the proposed control scheme can be stated as follows:

1- The closed-loop control system must be stable with some mild and easy-to-achieve conditions against I) time delay uncertainties and II) model mismatches.

2- The slave output y_s has to follow the master output y_m with arbitrary motion scaling K_p, which is called position tracking. Notice that the master and the slave outputs can be considered either position or velocity.

3- The reflecting force F_r has to follow the operator force F_h with arbitrary force scaling K_f, which is called force tracking.

These goals, in this paper, are achieved by designing two local controllers: one in the remote site C_s and the other in the local site C_m. These controllers are named the local slave and the local master controllers, respectively (Figure 1). The local slave controller guarantees the motion tracking. The local master controller guarantees the force tracking as well as the stability of the overall system. In the next sections, design of the local controllers is described.

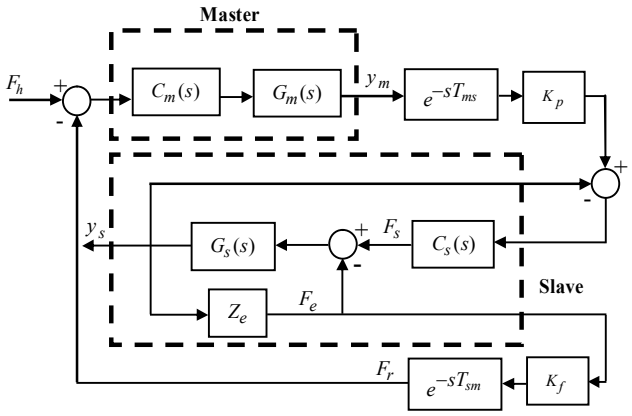

Figure 1. The basic proposed control scheme (the first form).

3. Controllers Design

In this section, design of the local controllers is presented. It should be mentioned that the designer can select arbitrary values for motion/force scaling.

3.1. The Local Slave Controller

Design of the local slave controller is based on the compliance control method. This means that force measurements are used at the remote site [1]. According to Figure 1, if the output of the master and the slave robots is position, then the transfer function from the slave to the master can be written as

$$\frac{X_s(s)}{X_m(s)} = \frac{K_p C_s(s) G_s(s)}{1 + Z_e G_s(s) + C_s(s) G_s(s)} e^{-sT_{ms}} . \tag{1}$$

Since the forward time delay does not appear in the denominator, the transfer function in Equation (1) is finite dimensional. Hence, the time delay will not have any effect on the stability of the system. In addition, one can use the classical control methods (such as PD) to design a local slave controller C_s for the remote site such that the system in (1) is stable. Therefore, the position of the slave robot will follow the position of the master robot in such a way that the tracking error for the position converges to zero. The effects of the time delay will be addressed in the next section.

3.2. The Local Master Controller

The local master controller is designed based on the direct force-measurement force-reflecting control**.** This controller must assure stability of the closed-loop system as well as force tracking. The force tracking means that the reflecting force $f_r(t)$ has to follow the human operator force $f_h(t)$. First, the following variables are defined:

$$\hat{G}_s(s) = \frac{Z_e C_s(s)\, G_s(s)}{1 + Z_e G_s(s) + C_s(s)\, G_s(s)}, \tag{2}$$

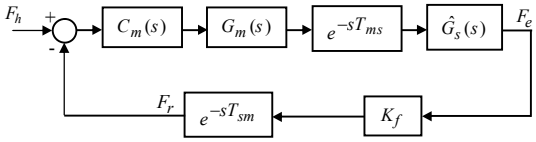

Figure 2. The second form of the proposed control scheme.

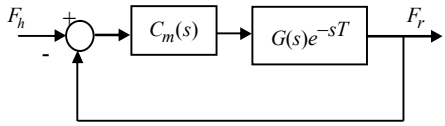

Figure 3. New control scheme (the third form).

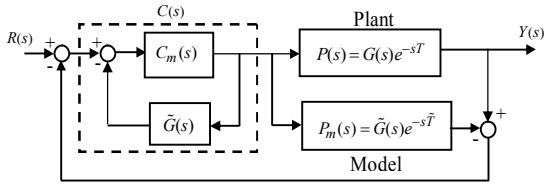

Figure 4. The Smith predictor control method.

$$M(s)=\frac{F_e}{F_h}=\frac{C_m(s)\,G(s)\,e^{-T_{ms}}}{1+C_m(s)\,G(s)\,e^{-(T_{ms}+T_{sm})s}}\,. \tag{4}$$

$$G(s)=\hat{G}_s(s)\;G_m(s)\,. \tag{3}$$

Using these variables, the control scheme, shown in Figure 1, can be simplified as in Figure 2. Notice that, the local slave controller C_s is designed such that poles of $\hat{G}_s$ are in the left-hand side of the *S*-Plane (i.e. C_s guarantees the position tracking). Then, the transfer function of the overall closed-loop system can be written from Figure 2 as

Now, since the force tracking is performed by sending the contact force through the reflection path of the communication channel, a new output in the block diagram of Figure 2 can be defined as F_r. This block diagram can be simplified as the block diagram in Figure 3. Using this block diagram, the transfer function of the overall closed-loop system can be written as

$$M(s)=\frac{F_r}{F_h}=\frac{K_f C_m(s)\,G(s)\,e^{-sT}}{1+C_m(s)\,G(s)\,e^{-sT}} \tag{5}$$

where $T=T_{ms}+T_{sm}$ and $F_r(s)=K_f F_e(s)\,e^{-sT_{sm}}$.

Notice that, the roles of $C_m(s)$ are to provide stability to the overall system and ensure the force tracking. From Equation (5), it can be seen that the time delay exists in the denominator of the closed-loop transfer function yielding an infinite dimensional transfer function. That is, the time delay can destabilize the system by reducing its stability margins or degrading its performance. As a result, one cannot use the classical control methods (like PD) to design a local master controller C_m such that the overall system in (5) is stable. Therefore, the fundamental problem in the proposed control method (i.e. the three different forms in Figs. 1, 2 and 3) is to cope with the time delay properly. The most popular and effective method to solve the time delay problem in a stable SISO process is the Smith predictor [23]. This predictor can effectively cancel out time

delays from the denominator of the closed-loop transfer function. In this way, one can use the classical control methods for the local master controller.

Figure 4 shows the block diagram of the Smith predictor. In this Figure, $P(s) = G(s)e^{-sT}$ denotes the transfer function of the plant, where G is a stable, strictly proper rational function, characterizing the delay-free part of the plant and T is a positive real number representing the time-delay. Moreover, $P_m(s) = \tilde{G}(s)e^{-s\tilde{T}}$ denotes the transfer function of the nominal model, where $\tilde{G}(s)$ and $\tilde{T}$ are the nominal version of $G(s)$ and T, respectively.

The main drawback of Smith predictor is its sensitivity to the process model. In other words, in Smith predictor: 1) the time delay must be constant and known a priori and 2) the model must be known precisely [24]. Hence, applications of Smith predictor are limited in teleoperation systems. To overcome these limitations, it is necessary to find a mechanism to compensate for time delay uncertainties and model mismatches. In the next section, the stability conditions for the closed-loop system will be discussed.

4. Stability Analysis

Stability of linear time-invariant (LTI) delay systems can be completely determined by the roots of its characteristic equation [25]. In this section, the stability analysis is performed for two cases: 1) Stability analysis due to the time-delay uncertainties, 2) Stability analysis due the model mismatches.

4.1. Stability Analysis for Time-Delay Uncertainties

In this part, stability of the proposed structure against the time-delay uncertainties is described. In order to avoid system instability due to the time-delay uncertainties, an adaptive filter is employed for predicting the time delay.

Figure 5 shows the structure of the local master controller. According to this Figure, the closed-loop transfer function is

$$M(s) = \frac{C_m(s)\, G(s) e^{-sT}}{1 + C_m(s)\, G(s) + C_m(s)\, G(s)\left[e^{-sT} - e^{-s\tilde{T}}\right]} \tag{6}$$

where $G(s)$ is defined in Equation (3). It is obvious that stability of the closed-loop system depends on the time delay. If the actual time delay T is equivalent to the estimated time delay $\tilde{T}$, then the closed-loop system is stable. In other words, if $T = \tilde{T}$ Equation (6) can be written as

$$M(s) = \frac{C_m(s)\, G(s) e^{-sT}}{1 + C_m(s)\, G(s)} \tag{7}$$

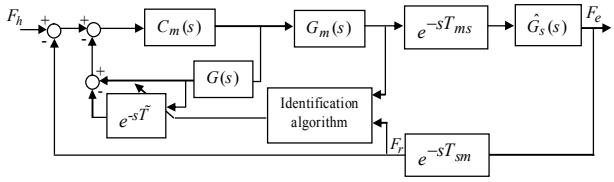

Figure 5. Structure of the local master controller.

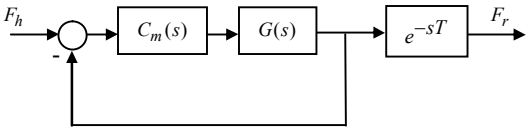

Figure 6. The desired control-loop configuration.

Figure 6 shows the block diagram of the equivalent closed-loop system for $T = \tilde{T}$. But due to the estimation errors $T \neq \tilde{T}$. Hence, the closed-loop system can become unstable.

Suppose, there exists estimation error for the time delay and let $\tilde{T} = T + \delta$ denote the estimated time delay. Then, the closed-loop transfer function, given in Equation (6), can be written as

$$M_\delta(s) = \frac{C_m(s)G(s)\ e^{-sT}}{1 + C_m(s)G(s) + C_m(s)G(s)\,e^{-sT}(1 - e^{-s\delta})}. \tag{8}$$

By considering the characteristic equation of (8), it is obvious that stability of the closed-loop system depends on the time delay. This fact can be shown as

$$\Delta_\delta(s) = 1 + C_m(s)\,G(s) + C_m(s)\,G(s)\,e^{-sT}(1 - e^{-s\delta}). \tag{9}$$

Now, the problem is to find the stability conditions such that the closed-loop system becomes stable. To do this, consider the no-delayed version of $G(s)$ and $C_m(s)$ as

$$G(s) = \frac{N_g(s)}{D_g(s)} \quad , \quad C_m(s) = \frac{N_c(s)}{D_c(s)}. \tag{10}$$

Then, the transfer function in (8) can be rewritten as

$$M_\delta(s) = \frac{N(s)\,e^{-sT}}{D(s) + N(s)\,e^{-sT}(1 - e^{-s\delta})}, \tag{11}$$

where polynomials $D(s)$ and $N(s)$ are equal to

$$D(s) = N_g(s)N_c(s) + D_g(s)D_c(s) \tag{12}$$

$$N(s) = N_g(s)N_c(s) \tag{13}$$

where it is assumed that $\deg(D(s)) > \deg(N(s))$ and polynomial $D(s)$ is Hurwitz.

In the following theorem, the condition for stability of the closed-loop system without any upper bound on the time delay will be shown.

THEOREM 1. *The closed-loop system in Figure 5 is independent of the estimated time delay* $\tilde{T}$ *, if*

$$\left|\frac{N(s)}{D(s)}\right|_{s=j\omega} < \frac{1}{2}, \quad \forall\omega.$$

where $D(s)$ *and* $N(s)$ *have are given in (12) and (13), respectively,* $D(s)$ *is Hurwitz,* $\deg(D(s)) > \deg(N(s))$, $N_g(s)$ *and* $D_g(s)$ *are the numerator and the denominator of the no-delay transfer function* $G(s)$, *respectively, and* $N_c(s)$ *and* $D_c(s)$ *are the numerator and the denominator of* $C_m(s)$, *respectively.*

Proof. The method of two-dimensional stability (2-D) test is used here for proof [26]. In this testing method, the system must be stable for $T = 0$ (i.e. stable for no time delay), which is true for the closed-loop system in Figure 5, since polynomial $D(s)$ is assumed to be Hurwitz.

Now, using the characteristic equation of the closed-loop system in (11), the equations for the 2-D test can be written as

$$\Delta_\delta(s) = D(s) + N(s)(z - \tilde{z}), \tag{14}$$

where $z = e^{-sT}$ and $\tilde{z} = e^{-s\tilde{T}}$,

$$\Delta_\delta(s, z, \tilde{z}) = 0, \tag{15}$$

$$\tilde{\Delta}_\delta(s, z, \tilde{z}) = \Delta_\delta(-s, z^{-1}, \tilde{z}^{-1}) = 0. \tag{16}$$

When no solution for (15) and (16) exists, then, according to the 2-D test, the closed-loop system must be stable. Using the characteristic equation, we have

$$\Delta_\delta(s, z, \tilde{z}) = D(s) + N(s)(z - \tilde{z}) = 0, \tag{17}$$

and

$$\begin{aligned} \tilde{\Delta}_\delta(s, z, \tilde{z}) &= \Delta_\delta(-s, z^{-1}, \tilde{z}^{-1}) \\ &= D(-s) + N(-s)(z^{-1} - \tilde{z}^{-1}) \\ &= z\tilde{z}D(-s) + N(-s)(\tilde{z} - z) = 0. \end{aligned} \tag{18}$$

From (17) we have

$$z = \tilde{z} - \frac{D(s)}{N(s)}. \tag{19}$$

Substituting (19) into (18) gives

$$\begin{aligned} \tilde{\Delta}_\delta(s, z, \tilde{z}) &= \Delta_\delta(-s, z^{-1}, \tilde{z}^{-1}) \\ &= \Delta_\delta\left(-s, \left[\tilde{z} - \frac{D(s)}{N(s)}\right]^{-1}, \tilde{z}^{-1}\right) \\ &= \tilde{z}\left[\tilde{z} - \frac{D(s)}{N(s)}\right]D(-s) + N(-s)\left[\frac{D(s)}{N(s)}\right] = 0. \end{aligned} \tag{20}$$

Hence,

$$\tilde{\Delta}_\delta(s, z, \tilde{z}) = \tilde{z}^2 N(s)D(-s) - \tilde{z}D(s)D(-s) + N(-s)D(s) = 0. \tag{21}$$

From there, it yields

$$\frac{N(s)}{D(s)}\tilde{z}^2 - \tilde{z} + \frac{N(-s)}{D(-s)} = 0\,, \tag{22}$$

The roots of (22) for $s = j\omega$ and $|\tilde{z}| = \left|e^{-j\omega\tilde{T}}\right| = 1$ must lie in the left-hand side of the *s*-plane. Substituting $\tilde{z} = e^{-j\omega\tilde{T}}$ and $s = j\omega$ into (22) gives

$$\frac{N(j\omega)}{D(j\omega)}e^{-2j\omega\tilde{T}} - e^{-j\omega\tilde{T}} + \frac{N(-j\omega)}{D(-j\omega)} = 0\,. \tag{23}$$

Factoring out $e^{-j\omega\tilde{T}}$ and noting that $\left| e^{-j\omega\tilde{T}} \right| \neq 0$, results into

$$e^{-j\omega\tilde{T}}\left[\frac{N(j\omega)}{D(j\omega)}e^{-j\omega\tilde{T}} - 1 + \frac{N(-j\omega)}{D(-j\omega)}e^{j\omega\tilde{T}}\right] = 0\,, \tag{24}$$

which gives

$$\frac{N(j\omega)}{D(j\omega)}e^{-j\omega\tilde{T}} + \frac{N(-j\omega)}{D(-j\omega)}e^{j\omega\tilde{T}} = 1\,. \tag{25}$$

Using the polar form, we have

$$\frac{N(j\omega)}{D(j\omega)}\left[\cos\omega\tilde{T} - j\sin\omega\tilde{T}\right] + \frac{N(-j\omega)}{D(-j\omega)}\left[\cos\omega\tilde{T} + j\sin\omega\tilde{T}\right] = 1 \tag{26}$$

Noting that in polar form, the magnitude is an even function, while phase is an odd function, one can conclude

$$2\left|\frac{N(j\omega)}{D(j\omega)}\right|\cos\left(\omega\tilde{T} + \measuredangle\frac{N(j\omega)}{D(j\omega)}\right) = 1 \tag{27}$$

Hence, the condition $|N(j\omega)/D(j\omega)| < 1/2$ is satisfied for all frequencies. Therefore, the characteristic equation of the closed-loop transfer function, given in (8), will not have any roots with positive real parts, which yields a stable system independent of $\tilde{T}$.□

Remark 1. In the proof of the above theorem, it was shown that the condition for stability of the closed-loop system, without any limit on the time delay, is

$$\left|N(j\omega)\Big/D(j\omega)\right| < \frac{1}{2}, \quad \forall\omega. \tag{28}$$

It is obvious that for a linear system it is always possible to design the local controllers such that: 1) they are stable, 2) the closed-loop system is transparent, and 3) the inequality (28) holds. Hence, using the proposed control method, stability can be assured.

Remark 2. In order to increase the robustness of the overall system, with uncertainties in time delays, one can design the local controller such that (28) is always valid. However, it should be noted that there exists a

trade off between $|N(j\omega)/D(j\omega)|$ and the precision of the transparency. That is, making this magnitude too small might compromise the transparency. This fact is true in practice as well; due to the existing delays in communication channel and uncertainties in the environment dynamics, there is a compromise between stability and transparency [20, 22]. In other words, transparency of the overall system can be improved without compromising the stability of the system, if the time delay is small enough. Based on this, Alfi et al. have proposed a theorem to relax the stability condition given in (28) for small time delays [21]. First, *small* time delay must be defined for teleoperation systems.

PROPOSITION 1: The time delay in communication channel in teleoperation systems is considered small for $T \le 0.001$ sec.

Proof: Brooks [27] proposed a bandwidth between 4 and 10 Hz for teleoperation systems. Consequently, by using the following first-order approximation for time delay in Laplace transform

$$e^{-sT} = 1 - sT \tag{29}$$

and also noting that $|e^{-T(j\omega)}| = |1 - T(j\omega)| = \sqrt{1+T^2\omega^2} \cong 1$, it gives $T = 0.001$ sec. Therefore, when it is referred to small time delay in communication channel, it means a time delay approximately less than or equal to 0.001 sec.

THEOREM 2. *Let $\delta = \tilde{T} - T$ denote the estimation error for the time delay. Then, the proposed control system, shown in Figure 6, is stable for small time delays if*

$$\left|\frac{N(s)}{D(s)}\right|_{s=j\omega} < 1, \quad \forall \omega,$$

where $D(s)$ and $N(s)$ have are given in (12) and (13), respectively, $D(s)$ is Hurwitz, $\deg(D(s)) > \deg(N(s))$, $N_g(s)$ and $D_g(s)$ are the numerator and the denominator of the no-delay transfer function $G(s)$, respectively, and $N_c(s)$ and $D_c(s)$ are the numerator and the denominator of $C_m(s)$, respectively.

Proof. Using the first-order approximation for e^{-Ts} and $e^{-\tilde{T}s}$ yields

$$e^{-sT} = 1 - sT, \quad e^{-s\tilde{T}} = 1 - s\tilde{T}. \tag{30}$$

Substituting (30) into the characteristic equation (9) gives

$$\begin{aligned}\Delta_\delta(s) &= 1 + C_m(s)G(s) + C_m(s)G(s)(e^{-sT} - e^{-s\tilde{T}}) \\ &= 1 + C_m(s)G(s) + C_m(s)G(s)(1 - sT - 1 + s\tilde{T}) \\ &= 1 + C_m(s)G(s) + C_m(s)G(s)(s\tilde{T} - sT) \\ &= 1 + C_m(s)G(s)[1 - s(T - \tilde{T})] \\ &= 1 + C_m(s)G(s)\, e^{-s(T-\tilde{T})}.\end{aligned} \tag{31}$$

Substituting $G(s) = N_g(s)/D_g(s)$ and $C_m(s) = N_c(s)/D_c(s)$ into (31) gives

$$\begin{aligned}\Delta_\delta(s) &= 1 + C_m(s)\, G(s)\, e^{-s(\tilde{T}-T)} \\ &= D(s) + N(s)\, e^{-s(T-\tilde{T})}.\end{aligned} \tag{32}$$

Using (31), (32) and $\delta = \tilde{T} - T$, Equation (8) can be rewritten as

$$M_\delta(s) = \frac{N(s)\, e^{-s\delta}}{D(s) + N(s)\, e^{-s\delta}}\; e^{-s(T-\delta)} \tag{33}$$

Since $e^{-s(T-\delta)}$ doesn't play any role in the stability of the closed-loop system, according to the Tsypkin theorem [28] the condition for the closed-loop stability is

$$\left| N(s)/D(s) \right|_{s=j\omega} < 1, \quad \forall \omega. \tag{34}$$

o

Remark 3. In the proof of the above theorem, it was shown that the condition for stability of the closed-loop system with small time delay in communication channel is

$$\left| N(j\omega)/D(j\omega) \right| < 1, \quad \forall \omega. \tag{35}$$

Obviously, for a linear system, it is always possible to design the local controllers such that: 1) they are stable, 2) the closed-loop system is transparent, and 3) the inequality (35) holds. Hence, using the proposed control method, stability can always be assured for small time delay in communication channel [20].

Remark 4. It should be noted that the condition given in (35) for small time delays does not have any conflict with the results of Theorem 1, given in (28). In other words, if condition (28) is satisfied, then (35) is guaranteed as well. This is because in the proof of Theorem 3, the time delay was assumed to be small, which imposes more restriction on the time delay but less restriction on the design of the local controllers.

Remark 5. Based on remark 2, if (35) is considered with small time delay, then, the robustness of the closed-loop system will be improved considerably against small time delay, but the transparency of the system might be compromised.

In the next section, the effects of the model mismatch on the stability of the proposed method will be addressed.

4.2. Stability Analysis Against Model Mismatches

In this section, the stability of the closed-loop system against model mismatches is investigated. It is well known that robot manipulators have nonlinear dynamics. On the other hand, since telemanipulators are modeled with linear dynamics in this paper, there is a model mismatch between the reality and the proposed method. Moreover, there are uncertainties in the task environment. In addition, the time delay uncertainty, which was addressed in the previous section, can also be considered as a model mismatch.

According to Figure 4

$$C(s) = \frac{C_m(s)}{1 + C_m(s)\tilde{G}(s)}, \tag{36}$$

$$P(s) = G(s)e^{-sT}, P_m(s) = \tilde{G}(s)e^{-s\tilde{T}}. \tag{37}$$

$$M(s) = \frac{Y(s)}{R(s)} = \frac{C_m(s)P(s)}{1 + C_m(s)[\tilde{G}(s) - P_m(s) + P(s)]} \tag{38}$$

It is obvious that stability of the closed-loop system depends on the model mismatch. This fact can be shown by considering the characteristic equation of the closed-loop system as

$$\Delta_\delta(s) = 1 + C_m(s)[\tilde{G}(s) - P_m(s) + P(s)] \tag{39}$$

Assuming that there is no model mismatch, i.e. $P(s) = P_m(s)$, we have

$$M(s) = \frac{Y(s)}{R(s)} = \frac{C_m(s)P_m(s)}{1 + C_m(s)\tilde{G}(s)} \tag{40}$$

Now, suppose there are model mismatches and let the model uncertainty be represented by some multiplicative perturbations $\delta(s)$. Then, the transfer function of the plant with uncertainties can be written as

$$P(s) = P_m(s)(1 + \delta(s)) \tag{41}$$

Without any loss of generality, if the norm of the model uncertainties is bounded, then, according to the following Theorem, the closed-loop system in Figure 4 is stable.

THEOREM 3. *The controller $C_m(s)$ provides robust stability if and only if*

$$\left\| \delta(j\omega)M(j\omega) \right\|_\infty < 1, \quad \forall\omega$$

A necessary and sufficient condition for robust performance is

$$\left\| \left| \delta(j\omega)M_c(j\omega) \right| + \left| F_w(j\omega)M_s(j\omega) \right| \right\|_\infty < 1, \quad \forall\omega$$

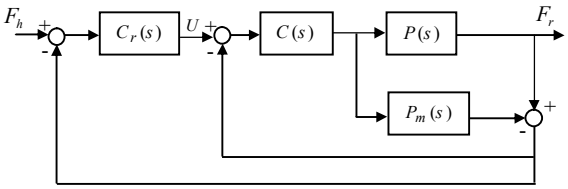

Figure 7: Equivalent of the Smith Predictor Scheme.

where M_c *is the complementary sensitivity transfer function,* M_s *is the sensitivity function of the closed-loop system,* $M_s(j\omega) = 1 - M_c(j\omega)$*, and* F_w *is the weighting function (the performance weight).*

Proof. See reference [29].

As it was mentioned earlier, the master controller guarantees stability and full transparency, when there is only time delay uncertainty. Now, since there are model mismatches as well (i.e. both the time delay uncertainties and the model parameter uncertainties exist), a robust term will be added to the control law. First, a procedure should be developed to convert the block diagram of Figure 4 to the block diagram in Figure 7 and vice versa as follows:

$$C(s) = \frac{C_m(s)}{1 + C_m(s)\,\tilde{G}(s)} \tag{42}$$

$$C_m(s) = \frac{C(s)}{1 - C(s)\,\tilde{G}(s)} \tag{43}$$

In Figure 7, the closed-loop transfer function can be written as

$$G_{ry}(s) = \frac{Y(s)}{R(s)} = \frac{C(s)P(s)}{1 + [P(s) - P_m(s)]C(s)}\,. \tag{44}$$

According to the control system theory, the ideal control would be realized if

$$Y(s) = R(s)\,. \tag{45}$$

As a result, the following conditions must be satisfied to have an ideal control system:

$$P(s) = P_m(s) \tag{46}$$

$$C(s)P(s) = 1 \tag{47}$$

The simple design procedure for $C(s)$ can then be stated as [30]

$$C(s) = P_m^{-1}(s)F(s)\,, \tag{48}$$

where

$$F(s) = \frac{1}{(\tau s + 1)^n}\,, \tag{49}$$

in which $F(s)$ is a low pass filter, and τ and n denote the filter time constant and the order of the filter, respectively.

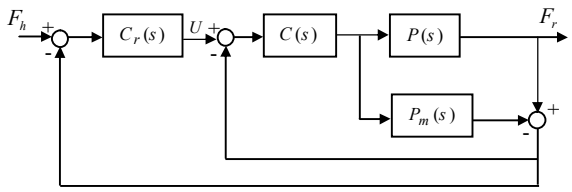

Figure 8. New robust control structure.

The order of the filter must be selected such that the controller $C(s)$ is realizable. In addition, theoretically, τ is selected such that an optimal compromise between the performance and the robustness is reached [31]. Zhang et al. have proposed a simple quantitative tuning procedure for this purpose [31]. In their procedure, τ can be selected as αT, where $T = T_{ms} + T_{sm}$. The larger the parameter α, the worse the nominal performance and the better the robustness. The range for α is from 0.1 to 1.2.

By considering Equation (48) for designing the controller, a precise model is needed. But in practice, it is hard to get the precise model for teleoperation systems. Hence, it is important to consider the model mismatches in stability analysis. The new structure for robustness against the model mismatches is shown in Figure 8.

In this Figure, the closed-loop transfer function from F_r to U can be written as

$$G_{uy}(s) = \frac{Y(s)}{U(s)} = \frac{C(s)\,P(s)}{1 + [P(s) - P_m(s)]\,C(s)} \tag{50}$$

Notice that, the above equation is equal to the closed-loop transfer function given in Equation (44). The goal is to design the robust controller $C_r(s)$ to cope with the model mismatches in Figure 8. The following Theorem provides the required conditions for the robust controller.

THEOREM 4. *Consider the closed-loop control system in Figure 8. Suppose the norm of uncertainties is defined as*

$$\left\|\delta(j\omega)\right\| = \left\|\frac{P_m(j\omega)}{P(j\omega)} - 1\right\| \le \gamma \quad , \quad \forall\omega$$

where $P(s)$ and $P_m(s)$ are the plant and the model given in (37), respectively. Then, according to the small-gain theorem, the controller $C_r(s)$ in Figure 8 provides robust stability if

$$\left\|\tilde{\delta}(j\omega)M(j\omega)\right\|_\infty < 1$$

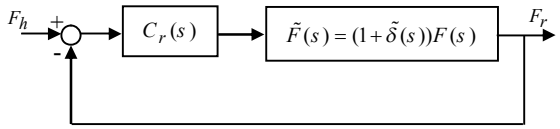

Figure 9. The equivalent block diagram of Figure 8.

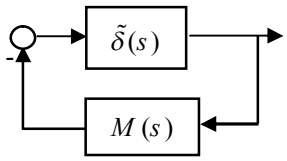

Figure 10. The equivalent of Figure 9.

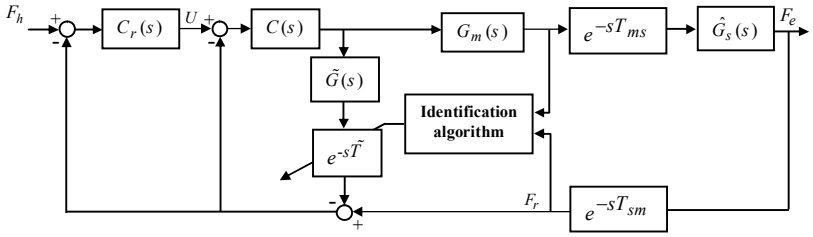

Figure 11. The structure design against model mismatch.

where $C(s)$ *and* $F(s)$ *are defined in (48) and (49), respectively,* $M(s) = \dfrac{C_r(s)F(s)}{1+C_r(s)F(s)}$ *is Hurwitz, (i.e. the closed-loop system is stable without model mismatches), and* $\tilde{\delta}(s) = \dfrac{-\delta(s)[1-F(s)]}{1+\delta(s)[1-F(s)]}$.

Proof. Substituting (48) into (50) gives

$$G_{uy}(s) = \frac{F(s)}{\dfrac{P_m(s)}{P(s)} + \dfrac{[P(s)-P_m(s)]}{P(s)}F(s)} \tag{51}$$

If we consider the model uncertainties by some multiplicative perturbations $\delta(s)$ as

$$P_m(s) = P(s)(1+\delta(s)), \tag{52}$$

then, (51) can be rewritten as

$$G_{uy}(s) = \frac{F(s)}{1+\delta(s)[1-F(s)]}. \tag{53}$$

Let us define the following new bounded variable:

$$\tilde{\delta}(s) = \frac{-\delta(s)[1-F(s)]}{1+\delta(s)[1-F(s)]}. \tag{54}$$

Using (54), (53) can be simplified as

$$G_{uy}(s) = F(s)(1+\tilde{\delta}(s)) \tag{55}$$

It is apparent that if there exists any model mismatch, then $\delta(s) \neq 0$ and consequently $\tilde{\delta}(s) \neq 0$. Hence, if $\delta(s)$ is bounded, $\tilde{\delta}(s)$ is bounded as well. On the other hand, $\|\delta(s)\|_\infty \leq \alpha$ yields $\left\|\tilde{\delta}(s)\right\|_\infty \leq \beta$, where α and β are some positive numbers. Equation (55) demonstrates that the model mismatch can be represented by uncertainties in the

filter $F(s)$. Consequently, Figure 8 is equivalent to Figure 9, and then equivalent to Figure 10. Hence, according to the small-gain theorem [32], the closed-loop system in Figure 10 is robust stable if and only if

$$\left\| \tilde{\delta}(s)M(s) \right\|_{\infty} < 1, \tag{56}$$

where $M(s) = \dfrac{C_r(s)F(s)}{1 + C_r(s)F(s)}$ is Hurwitz. I.e. the closed-loop system is stable without any model mismatches.o

Remark 6. By considering (56), it is apparent that the smaller the value of $\left\| \tilde{\delta}(j\omega)M(j\omega) \right\|_{\infty}$, the higher the robustness for the overall system against model mismatches. However, there exists a trade off between $\left\| \tilde{\delta}(j\omega)M(j\omega) \right\|_{\infty}$ and the transparency. That is, making this magnitude too small might compromise the transparency.

Figure 11 shows the modified block diagram of the proposed structure, shown in Figure 1, against model mismatches.

5. Simulations

The dynamic equation of the master and the slave systems are considered here as a single-link manipulator by [33]

$$(J_m s^2 + B_m s + M_m g L_m)\theta_m = u_m, \quad (J_s s^2 + B_s s + M_s g L_s)\theta_s = u_s$$

where J, M and L are the moment of inertia, the mass, and the length of the manipulators links, respectively; B is the viscous friction coefficient, θ is the rotational angle, g is the gravity acceleration, and u is the input; indices m and s are for the master and the slave, respectively. The system parameters are set to $J_m = 2$ kg.m^2, $B_m = 3$ N/m, $L_m = 0.2$ m, and $M_m = 0.6$ kg for the master, $J_s = 1$ kg.m2, $B_s = 5$ N/m, $L_s = 0.3$ m, and $M_s = 2$ kg for the slave, and Z_e =1 for the environment impedance. Moreover, the position and the force scalings are set equal to 0.2 and 4, respectively. In order to demonstrate performance of the proposed methods, simulations are carried out for two cases: 1) the time delay uncertainties (section 4.1) and 2) the model mismatches (section 4.2). In addition, normally distributed random signals are used as uncertainties in the time delay. The time delay is estimated with an FIR filter [34]. Order of the FIR filter is selected as $P = 6$, because as it is mentioned in [34] for $P \geq 6$ the estimation error of the time delay will be very small and negligible.

In simulations, three different controllers are designed. The first controller is a PD controller, called the local slave controller C_s, which is used for the remote site. The second controller is a PD controller, called the local master controller C_m, which is used for the local site. The third controller is a robust controller, which is used for the local site. Notice that the latest controller is only required for model mismatches. The slave controller is designed such that

$\hat{G}(s)$ is stable, and the master controller is designed such that the goals of the closed-loop teleoperation system is satisfied. Moreover, the master controller is designed such that the robust stability condition against time delay uncertainties, given in (28) and (35), is also achieved. Finally, the robust controller is designed such that the robust stability condition against model mismatches, given in (56), is achieved.

5.1. Time Delay Uncertainties

Simulations for the time delay uncertainties are carried out for different values of the time delay. In case I, the time delay is small with some perturbations, while in case II the time delay is relatively large with considerable perturbations. Simulations for the time delay uncertainties are shown in Figures 12-20**.** Figures 12 and 16 represent the time delay for the cases I and II, respectively, where $T = T_{ms} + T_{sm}$. In addition, Tables 1 and 2 show the type of the local controllers and their typical coefficients used in cases I and II, respectively. Notice that, these values are not unique and are selected only to satisfy the stability conditions given in Equations (28) and (35). The stability conditions can be checked using the Bode plot given in Figures 13 and 17. The dashed line in Figures 13 and 17 represent the right-hand side of Equations (28) and (35) (i.e. $20\log(0.5) \cong -6$ db and $20\log(1) = 0$ db), respectively. Figures 14-15 and 18-19 represent the transparency response for the step and the sinusoidal inputs. As these figures show, the proposed method can cope very well with time delay uncertainties. Notice that, the stability conditions in these cases, given in (28) and (35), cannot cope with model uncertainties (Figure 20). This Figure confirms the instability of the teleoperation system against model uncertainty, where 20% and 25% parametric uncertainty are assumed for the viscous friction in the master-slave and the environment impedance, respectively.

Table 1. Type of the master controllers

Case	Local Controller	K_P	K_D
Case I	PD	1.25	0.15
Case II	PD	1	2.5

Table 2. Type of the slave controllers

Case	Local Controller	K_P	K_D
Case I	PD	20	34.8
Case II	PD	20	34.8

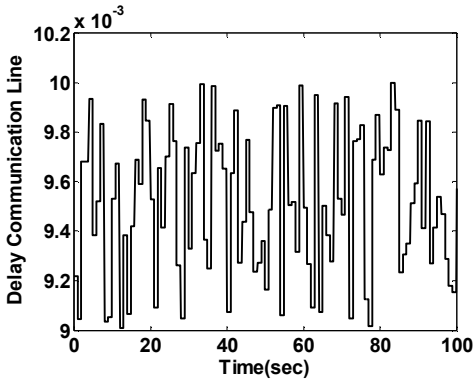

Figure 12. Time delay in communication channel (case I), where $T = T_{ms} + T_{sm}$.

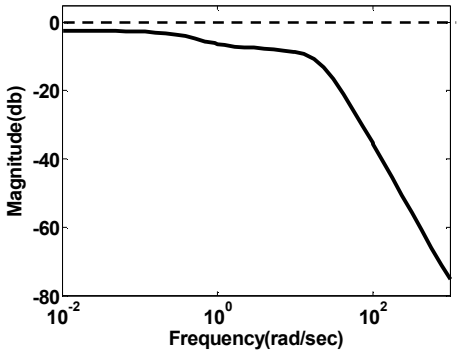

Figure 13. Bode plot for presenting stability condition in Equation (45), (case I).

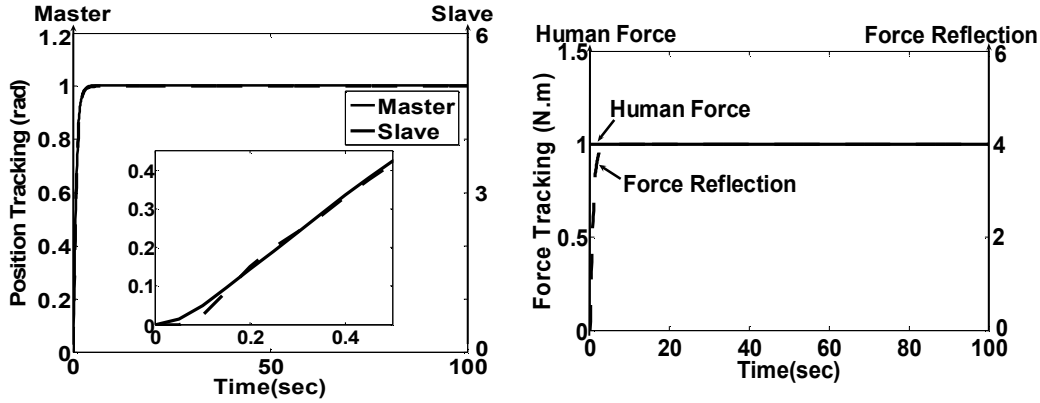

Figure 14. Transparency response for step input (case I).

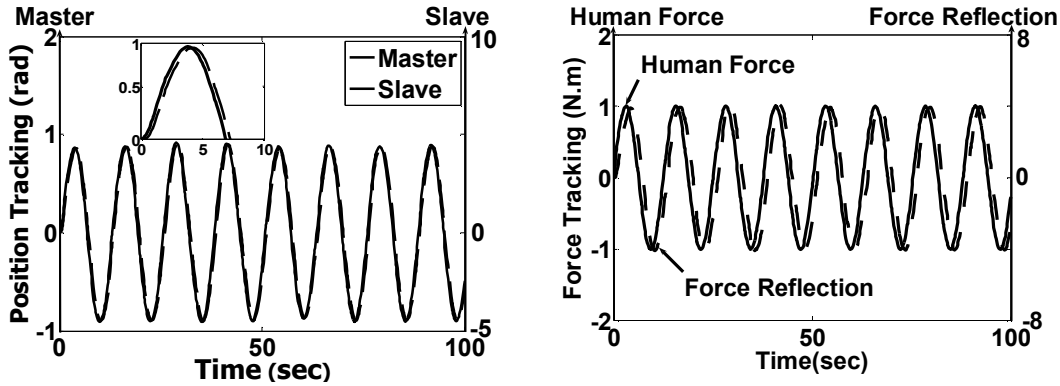

Figure 15. Transparency response for sinusoidal input (case I).

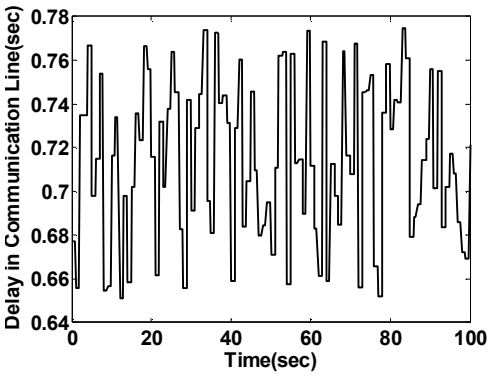

Figure 16. Time delay in communication channel (case II), where $T = T_{ms} + T_{sm}$

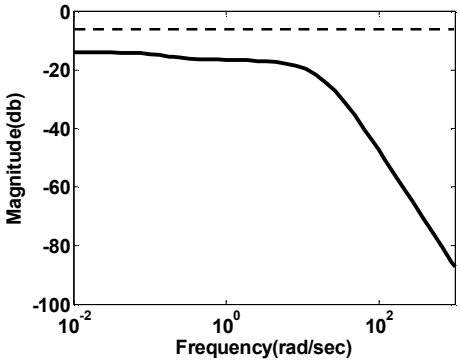

Figure 17. Bode plot for verifying the stability condition in Equation (28), (case II)

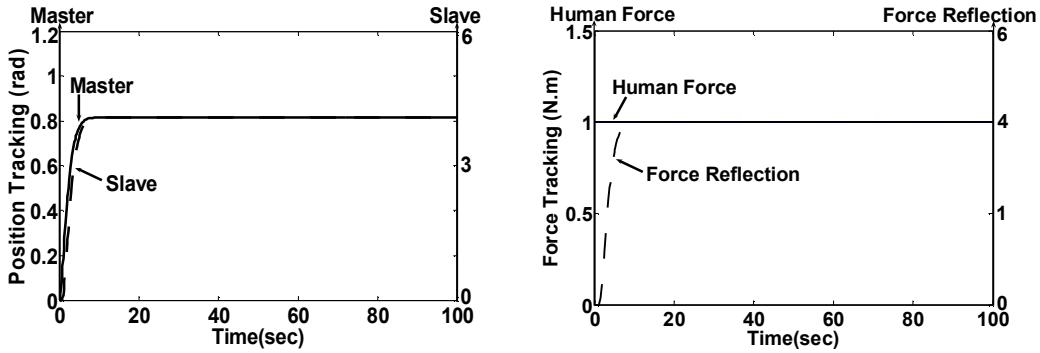

Figure 18. Transparency response for step response, case (II).

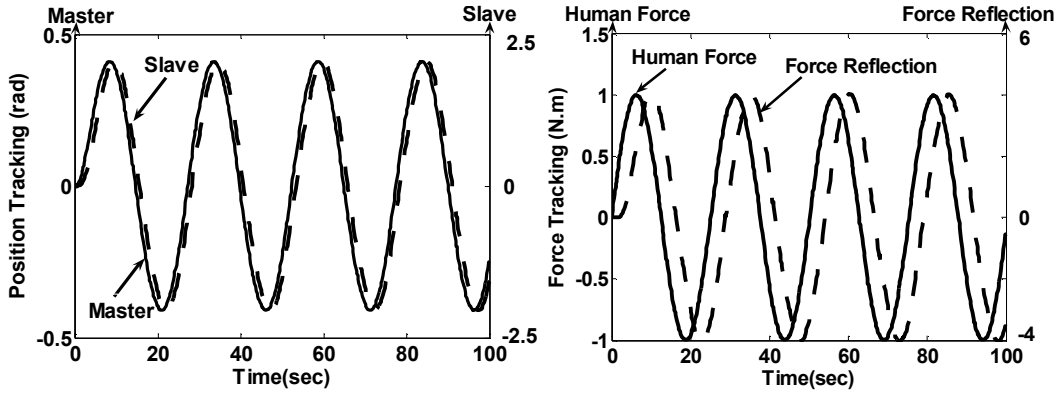

Figure 19. Transparency response for sinusoidal response, case (II).

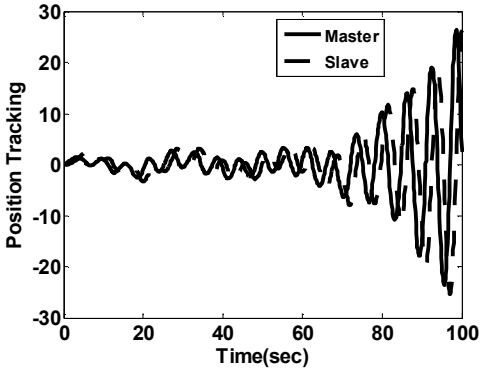

Figure 20. Unstable response, when some model mismatches are introduced.

5.2. Model Mismatches

In order to evaluate the effectiveness of the proposed method against model mismatches, parameter uncertainties in the master, the slave and the task environment, as well as the time delay uncertainties are considered here. The following nonlinear equation represents the dynamic equation for the master and the slave robots

$$J\ddot{\theta} + B\dot{\theta} + K\sin\theta = u\,.$$

Moreover, 20% and 25% are added as extra uncertainties to the viscous friction of the master-slave and the environment impedance, respectively. In addition, the time delay uncertainty, shown in Figure 12, is considered in the communication channel.

The selected values for the controllers are $K_P = 2.5$ and $K_D = 1$ for the slave controller, and $K_P = 0.25$ and $K_D = 0.05$ for the master controller. Moreover, the robust controller is selected as $C_r = 1/(10s+1)$. Notice that, these numerical values are not unique and are selected only to satisfy the performance and the stability conditions. The order of the low pass filter, $F(s)$ in (49), is equal to three. Recall that, the order of the low pass filter must be selected such that the robust controller is realizable. Furthermore, for the time constant of the low pass filter ($\tau = \alpha T$), where $T = T_{ms} + T_{sm}$, the parameter α is set to 0.5 (see Section 4.2 for details).

Figure 21 shows the Bode plot to verify the stability condition given in (56). The dashed line in this Figure represents the right-hand side of Equation (56) (i.e. 20log(1)=0 db). Notice that, Remark 6 is considered here. Figures 22 and 23 illustrate the transparency response of the proposed control method for the step and the sinusoidal inputs, respectively. As these figures show, the proposed structure exhibits good performance for both the stability as well as the transparency of the scaled teleoperation system in presence of model mismatches. It should be noticed that the time delay in force tracking is more than the time delay in position tracking. This is due to the defined variables for the force tracking, in which the time delay is the sum of the forward and the backward time delays.

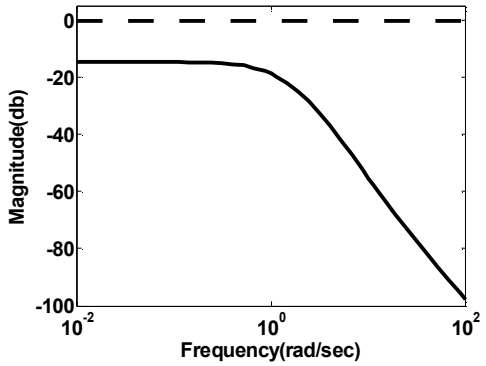

Figure 21. Bode plot for verifying the stability condition in (49).

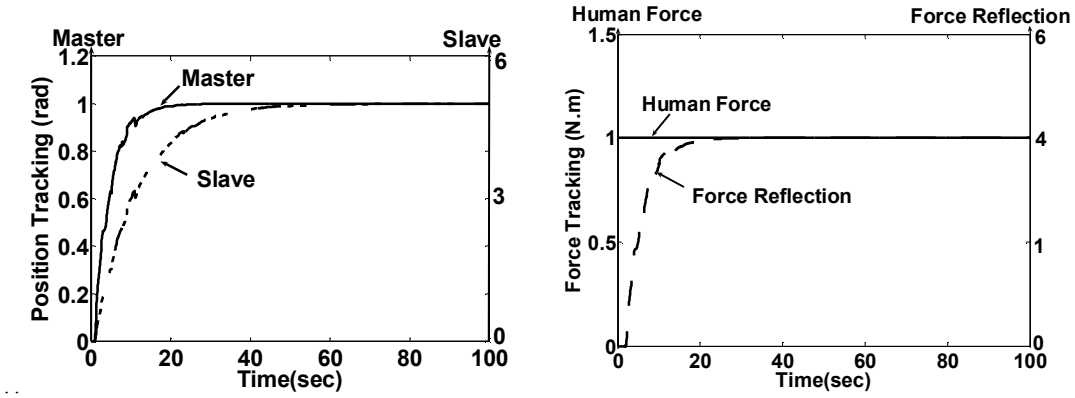

Figure 22. Transparency response for step input.

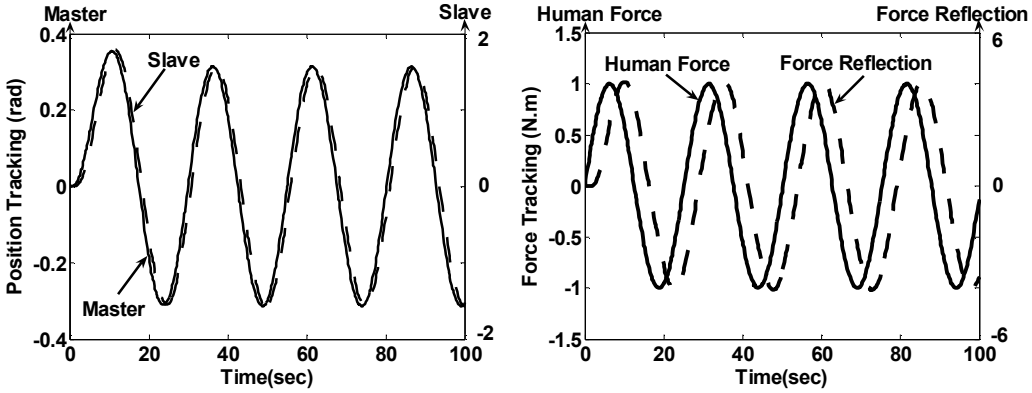

Figure 23. Transparency response for sinusoidal input

6. Conclusions

To achieve transparency and stability robustness against model mismatches in scaled teleoperation systems with arbitrary motion/force scaling, a simple control scheme was proposed in this paper. The model mismatches included uncertainties in the time delay in communication channel and model parameters uncertainties. In the proposed approach, three controllers were designed: Two local controllers, one for the master side, one for the slave side, and a robust controller. These controllers were designed such that the slave controller guarantees the motion tracking and the master controller guarantees the stability of the inner closed-loop system. The robust controller guarantees stability robustness against model mismatches. The major advantage of the proposed method was that one could use the classical control methods to design the local controllers as well as the robust controller. Furthermore, the controller design would be straightforward; these controllers only need to satisfy one simple condition. In simulations, for a one-degree-of-freedom manipulator example, it was shown that the proposed method is a viable choice for the teleoperation systems with model mismatches.

References

1. Melchiorri, C. and Eusebi, A.: Telemanipulation: System aspects and control issue, *in Proc. of the Modeling and Control of Mechanisms and Robots*, World Scientific, Singapore, 1996, pp. 149-183.

2. Sheridan, T. B.: Space telerobotic through time delay: review and prognosis, *IEEE Trans. Robotics Automat*. **9(5)** (1993), 592-606.

3. Lawrence, D. A.: Stability and transparency in bilateral teleoperation, *IEEE Trans. Robotics Automat*. **9(5)** (1993), 625-637.

4. Ferrell, W. R.: Remote manipulation with transmission delay*," IEEE Trans. Human Factors* **HFE-8** (1966), 24-32.

5. Vertut, J. and Coiffet, P.: *Telerobotic and Robotics: Evolution and Development*, Kogan Page Press, London, 1985.

6. Anderson, J. and Spong, M. W.: Bilateral control of teleoperators with time delay, *IEEE Trans. Automat. Control* **34**(5) (1989), 494-501.

7. Niemeyer, G. and Slotine, J. E.: Stable adaptive telerobotic, *IEEE J. Oceanic Engineering* **26**(1) (1991), 152-162.

8. Niemeyer, G. and Slotine, J. E.: Towards force-reflecting teleoperation over the internet, *IEEE international Conference on Robotics and Automation,* Leuven, Belgium, pp.1909-1915, 1997.

9. Kim, W. S., Hannaford, B., and Bejczy, A. K.: 1992, Force reflection and shared compliant control in operating telemanipulators with time delay, *IEEE Trans. Robotics Automat*. **8**(2) (1992), 176-185.

10. Buttolo, P., Braathen, P. and B. Hannaford: Sliding-Mode controller for bilateral teleoperation: Preliminary studies, *Presence* **3**(2) (1994), 158-152.

11. Grace a-Valdovinos, L. G., Parra-Vega, V. and Arteaga, M. A.: Higher-order sliding mode impedance bilateral teleoperation with robust estimation under constant unknown time delay, in: *Proc. of the IEEE/ASME International Conference on Advanced Intelligent Mechatronics*, Monterey, California, USA, 2005, pp. 1293-1298.

12. Leeraphan, S., Maneewarn, T. and Laowattana, D.: Stable adaptive bilateral control of transparent teleoperation through time-varying delay, in: *Proc. of the IEEE International Conference on Intelligent Robots and Systems*, 2003, pp. 2979-2983.

13. Zhu, W. H and Salcudean, S. E.: Stability guaranteed teleoperation: An adaptive motion/force control approach, *IEEE Trans. Automatic Control* **45**(11) (2000), 1951-1969.

14. Munir, S. and Book, W. J.: Internet-based telerobotic using wave variable with prediction, *IEEE/ASME Trans. Mechatronics* **7** (2002), 124-133.

15. Hashtrudi-Zaad, K., and Salcudean, S. E.: Transparency in time-delayed systems and the effect of local force feedback for transparent teleoperation, *IEEE Trans. Robotics Automat*. **18**(1) (2002), 101-114.

16. Yokokohji, Y. and Yoshikawa, T.: Bilateral control of master-slave manipulators for ideal kinesthetic coupling-formulation and experiment, *IEEE Trans. Robotics Automat*. **10**(5) (1994), 605-620.

17. Leung, G. M. H., Francis, B. A. and Apkarian, J.: Bilateral controller for teleoperators with time delay via μ -synthesis, *IEEE Trans. Robotics Automat.* **11**(1) (1995), 105-116.

18. Baier, H. and Schmidt, G.: Transparency and stability of bilateral kinesthetic teleoperation with time-delayed communication, *J. Intelligent Robotic Syst*. **40** (2004), 1-22.

19. Ching, H. and Book, W. J.: Internet-based bilateral teleoperation based on wave variable with adaptive predictor and direct drift control, *ASME J. Dynamic Systems, Measurement Control* **128** (2006), 86-9.

20. Alfi, A. and Farrokhi, M., Bilateral transparent telerobotic with long time-varying delay: new control design and stability analysis, in: *Proc. of the 45th IEEE Conference on Decision and Control CDC 2006*, San Diego, USA, 2006.

21. Alfi, A. and Farrokhi, M.: Bilateral control to achieve transparent telerobotic with perturbation of static time delay, in: *Proc. of the 32nd Annual Conf. IEEE Industrial Electronics Society IECON 2006*, Paris, France, 2006.

22. Alfi, A. and Farrokhi, M.: On the closed-loop stability analysis of transparent telerobotic systems with time-varying delay using a new structure, in: *Proc. of the 6th IFAC Workshop on Time Delay Systems TDS 2006*, L'Aquila, Italy, 2006.

23. Smith, O. J. M.: Closer control of loops with dead time, *Chem. Eng. Progress* **53**(5) (1957), 217-219.

24. Palmor, Z.: Stability properties of smith dead-time compensator controllers, *Internat. J. Control* **32** (1980), 937-949.

25. Kailath, T.: *Linear Systems, Prentice Hall*, New Jercy, 1990.

26. Gu, K., Kharitanov, V. L., and Chen, J.: *Stability of Time-Delay Systems*, Birkhauser, Stuttgart, 2003.

27. Brooks, T. L., *Teleoperator system response for nuclear telepresence*, STX Publication, ST System Corp, 1990.

28. Niculescu, S. I.: *Delay Effects on Stability: a Robust Control Approach*, Springer Verlarg, Heidelberg, 2001.

29. Doyle, J. C., Francis, B. A., and Tannenbaum, A. R.: *Feedback Control Theory*, Macmillan Pub. Co., New York, 1992.

30. Morari, M. and Zafiriou, E.: *Robust Process Control*, Prentice-Hall, Englewood Cliffs, New York, 1989.

31. Zhang, W., He, X., and Xu, X.: Comparison of several well-known controllers used in process control, *ISA Transactions* **42** (2003), 1-8.

32. Marquez, H. J.: *Nonlinear Control Systems: Analysis and Design*, Wiley-Inter Science, 2003

33. Hokayayem, P. F. and Spong, M. W.: Bilateral teleoperation: an historical survey, *Automatica* **42**(2006), 2035-2055.

34. Balestrino, A., Verona, F. B, and Landi, A.: Online process estimation by ANNs and Smith controller design, *IEE Control Theory and Application* **145**(2) (1998), 231-235.s